Supplemental Materials for

Large anionic liposomes enable targeted intraperitoneal delivery of a TLR 7/8 agonist to re-polarize ovarian tumors' microenvironment

Yanan Kang[1,2,4], Linda Flores[1], Hoi Wa Ngai[1], Yvonne R. Cornejo[1,2,4], Tom Haber[2], Marisa McDonald[1], Dayson Friaça Moreira[3], Joanna Marie Gonzaga[1], Wafa Abidi[2], Yijia Zhang[2], Mohamed Hammad[1], Marcin Kortylewski[3], Karen S. Aboody[1], Jacob M. Berlin[2]*

[1]Department of Developmental and Stem Cell Biology, [2]Department of Molecular Medicine, [3]Department of Immuno-Oncology, [4]Irell & Manella Graduate School of Biological Sciences Beckman Research Institute at City of Hope, 1500 East Duarte Road, Duarte, CA, 91010, United States

***CORRESPONDING AUTHOR**:

[*] Corresponding author

E-mail: jacobberlincoh@gmail.com

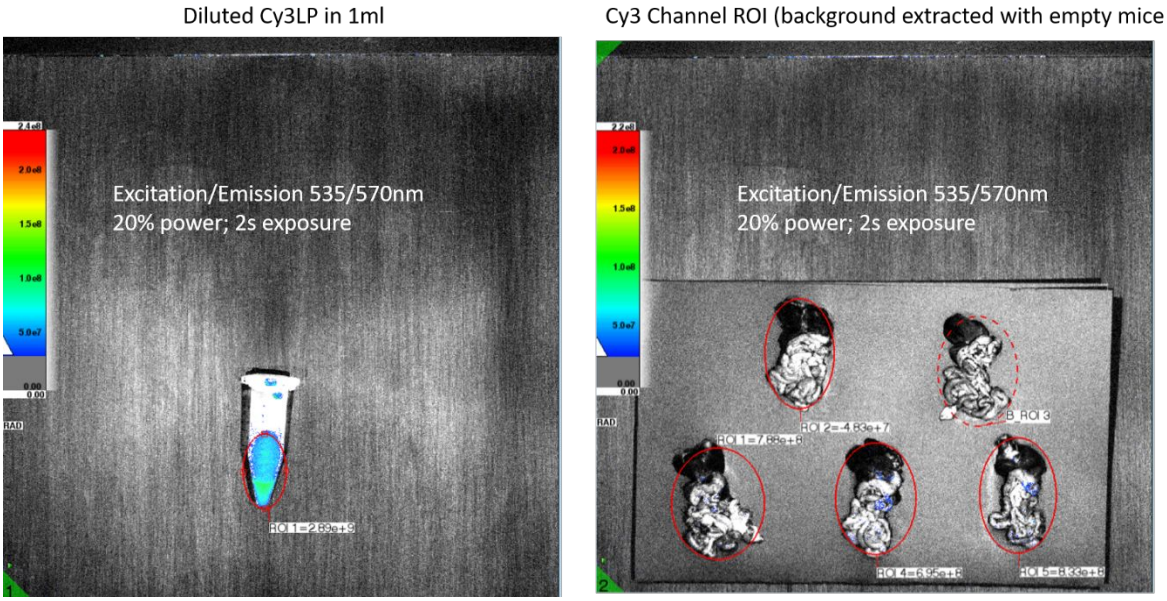

Figure S1. AmiX fluorescent characterization of injected Cy3LP. Cy3LP at injected volume were imaged first using Lago AmiX (excitation/emission = 535/570nm) with 20% excitation power and 2sec of exposure. Image on the right is the fluorescent image of IP pluck of euthanized animals injected with PBS (top) or Cy3LP (bottom) with same filter set and excitation power, region of interest (ROI) for PBS injected mice were used as background ROI.

a

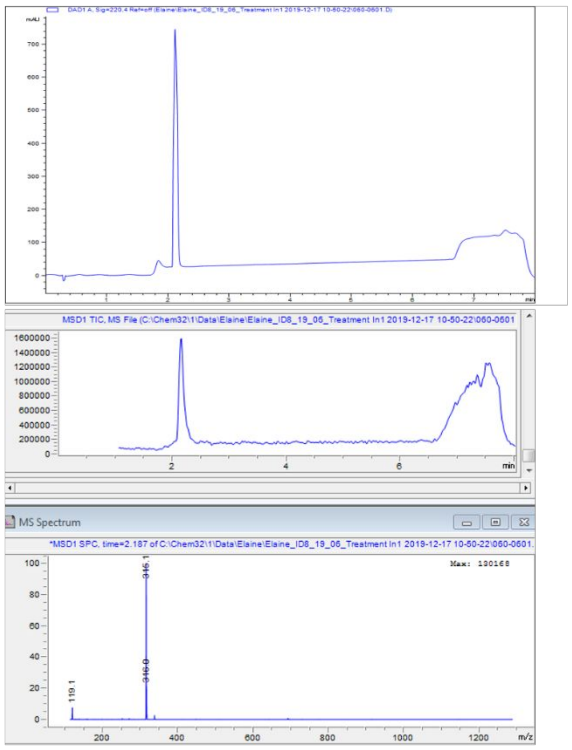

b

	Total Conc. (µg/ml)	Loaded Conc. (µg/ml)	Loading efficiency
DPPC Remote Loading #1	571.07	190.59	33.37
DPPC Remote Loading #2	585.62	152.62	26.06
DPPC Remote Loading #3	557.23	158.18	28.39
DPPC Remote Loading #4	567.87	141.97	25.00
DPPC Remote Loading #5	549.7	244.9	44.55
DPPC Conventional Loading		39.83	

Loading Optimization	Total Conc.	Loaded Conc.	Loading efficiency
DPPC 60C 1hr	563	188.7	34.00
DPPC 60C 2hr	487	161.8	33.00
DPPC 65C 1hr	522	174.2	33.00
DPPC 70C 1hr	578	194.1	34.00

	Area under the curve	Conc.
450ug_ml flowed through PD-10 column	26.5	-1.7

c

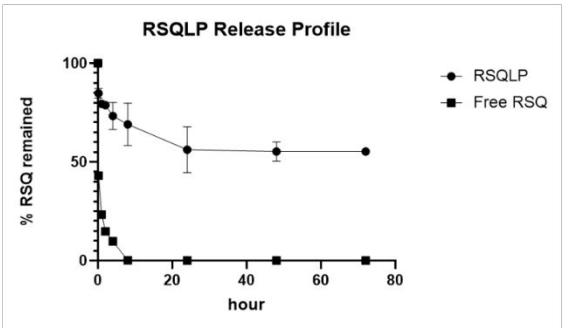

Figure S2. Loading optimization and consistency. a) HPLC chromatograph showing the peak of RSQ (220nm) and MS mass determination of selected peak eluted at 2.18 min (M.W 314). b) Five loading experiments were executed separately in order to investigate the loading consistency. RSQ were loaded using conventional passive loading method in order to validate the remote loading method. Loading conditions were probed with different temperature and time for optimum loading protocol. Purification process was validated by loading the same input RSQ to PD-10 column and collection of elution fraction. All RSQ concentrations were determined using HPLC-MS c) Liposome-RSQ *in vitro* release profile in comparison to free RSQ in same apparatus (100kDa dialysis cassette against x200 sample volume PBS). n=3

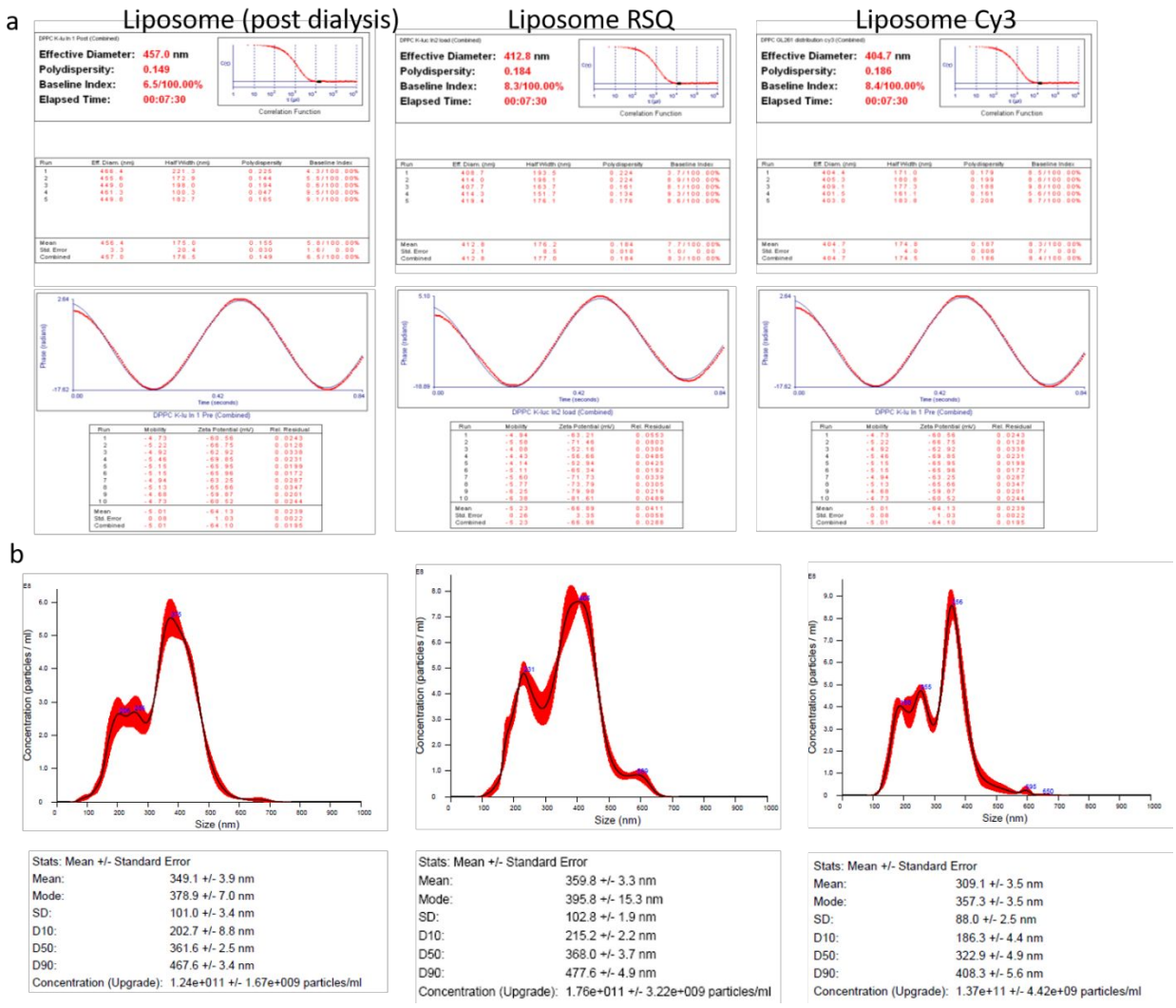

Figure S3. DLS, Zeta and Nanosight characterization of prepared liposomes. a) From left to right, DLS and Zeta potential for liposomes (post dialysis), Liposome RSQ and Liposome Cy3 reported in Figure 1d. b) Nanosight tracking analysis of prepared liposomes in the same order described in a).

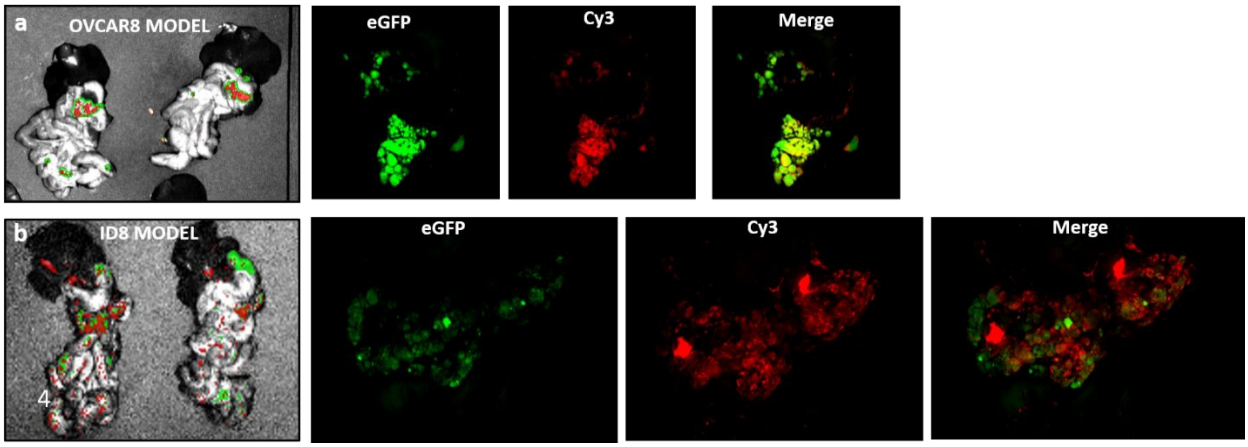

Figure S4. In vivo biodistribution of Cy3 liposomes in OVCAR8 bearing nude mice and ID8 bearing C57B6 mice. a. Fluorescent (amiX lago) overlay images showing *in vivo* biodistribution of Cy3LP after 24hr of IP administration (Green: OVCAR8.eGPF.ffluc; Red: Cy3LP). Subsequently showing the fluorescent macroscope images with a more zoomed view showing the green signal (eGFP) and red signal (Cy3LP) near omentum. b. Additional ID8.eGFP.ffluc bearing mice that were injected with Cy3LP and imaged at 24hr post IP injection. On the right showing the fluorescent macroscope images showing the localization of Cy3LP signals on omentum tumor. (Note: ID8.eGFP.ffluc tumor model have weak eGFP signal, the stomach are showing strong green signal)

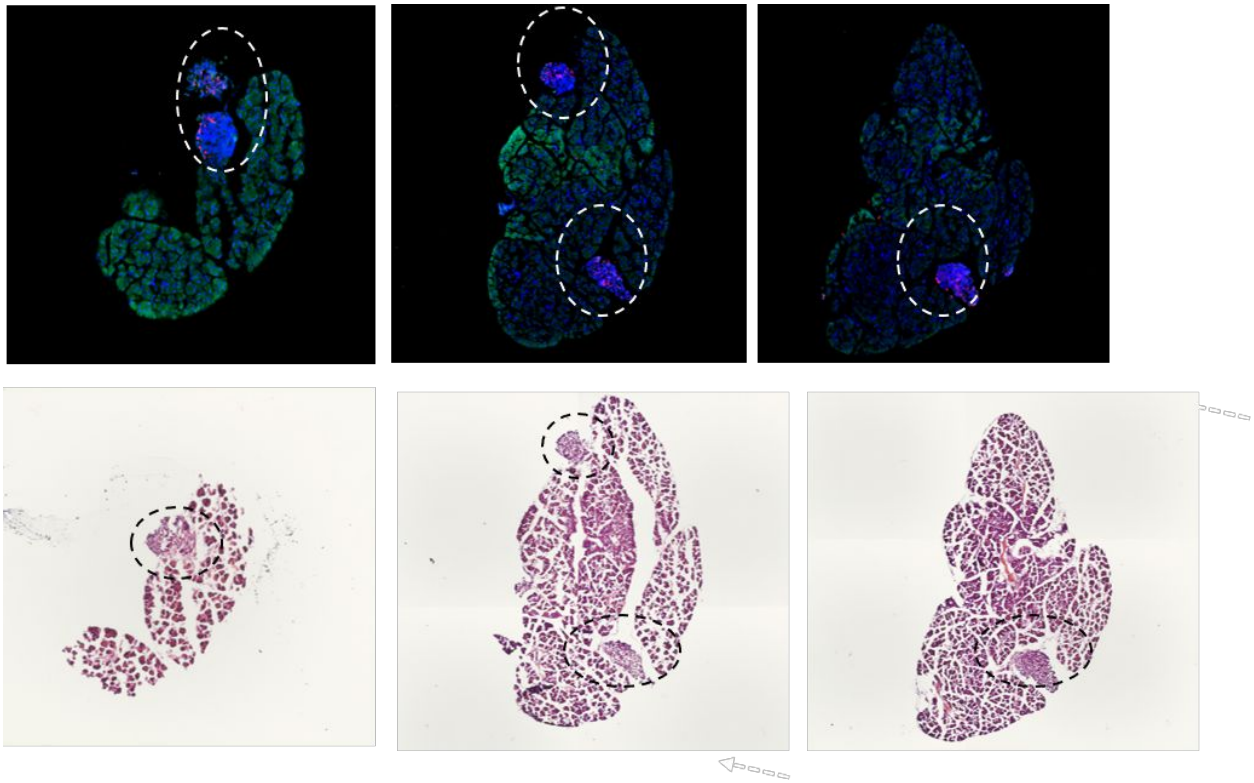

Figure S5. Cy3 liposomes label tumors around pancreases. Top. ID8 tumors from Figure S1b were collected, fixed and cryosectioned. Shown are light fluorescent images of adjacent slides of tumors around the pancreases (dotted circle tumor). Slides were stained with DAPI. Bottom. Adjacent slides that were stained with H&E showing normal tissue (pancreases) and tumor tissue (ID8 tumors).

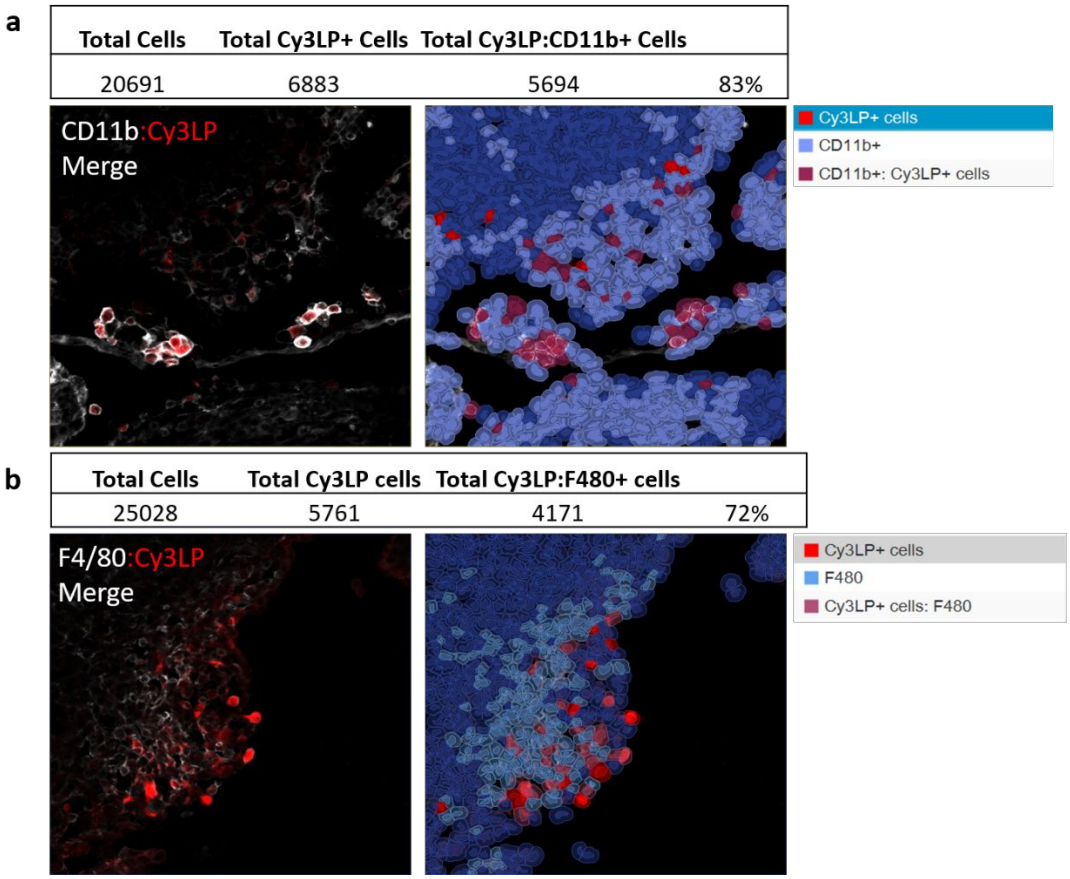

Figure S6. Quantitative analysis of Cy3LP distribution in collected ID8 tumors. a) b) representative images showing CD11b-(a) (white) F4-80-(b) (white), Cy3LP (red) and cell classification segmentation on the right (color keys are presented on the right).

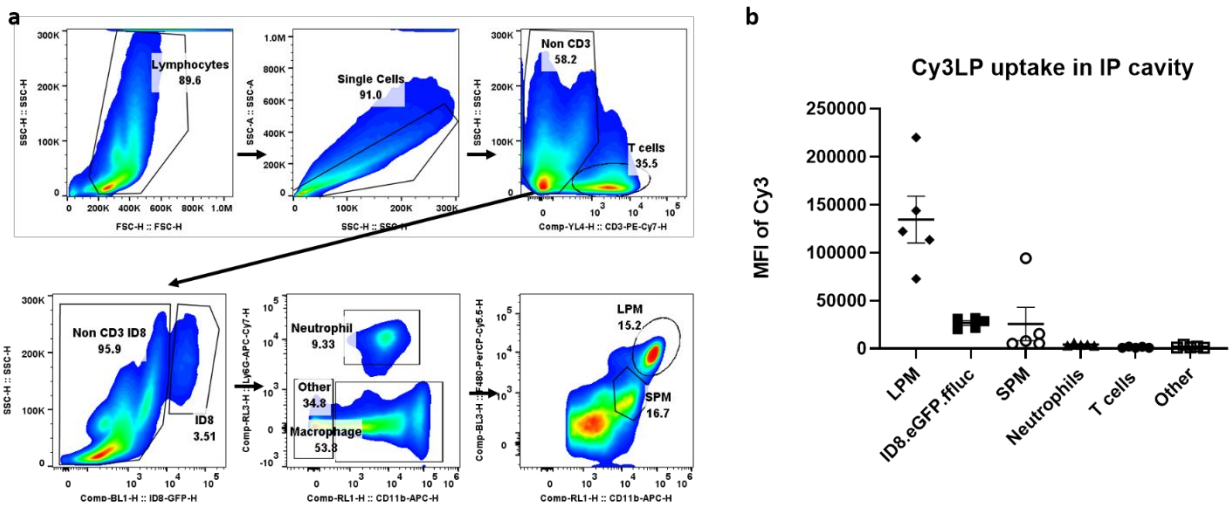

Figure S7: Cy3LP uptake to peritoneal cells 24hr post administration. Cy3LP were injected to ID8.eGFP.ffluc tumor bearing mice, peritoneal lavage fluid were collected. After red blood cell lysis, cells were stained with various antibodies (CD11b, F480, Ly6G, CD3). a) Gating strategy for stained samples. Large peritoneal macrophages (LPM) and small peritoneal macrophages (SPM).[1] b) MFI (Mean fluorescent intensity) of Cy3 (PE) channel for different cell types.

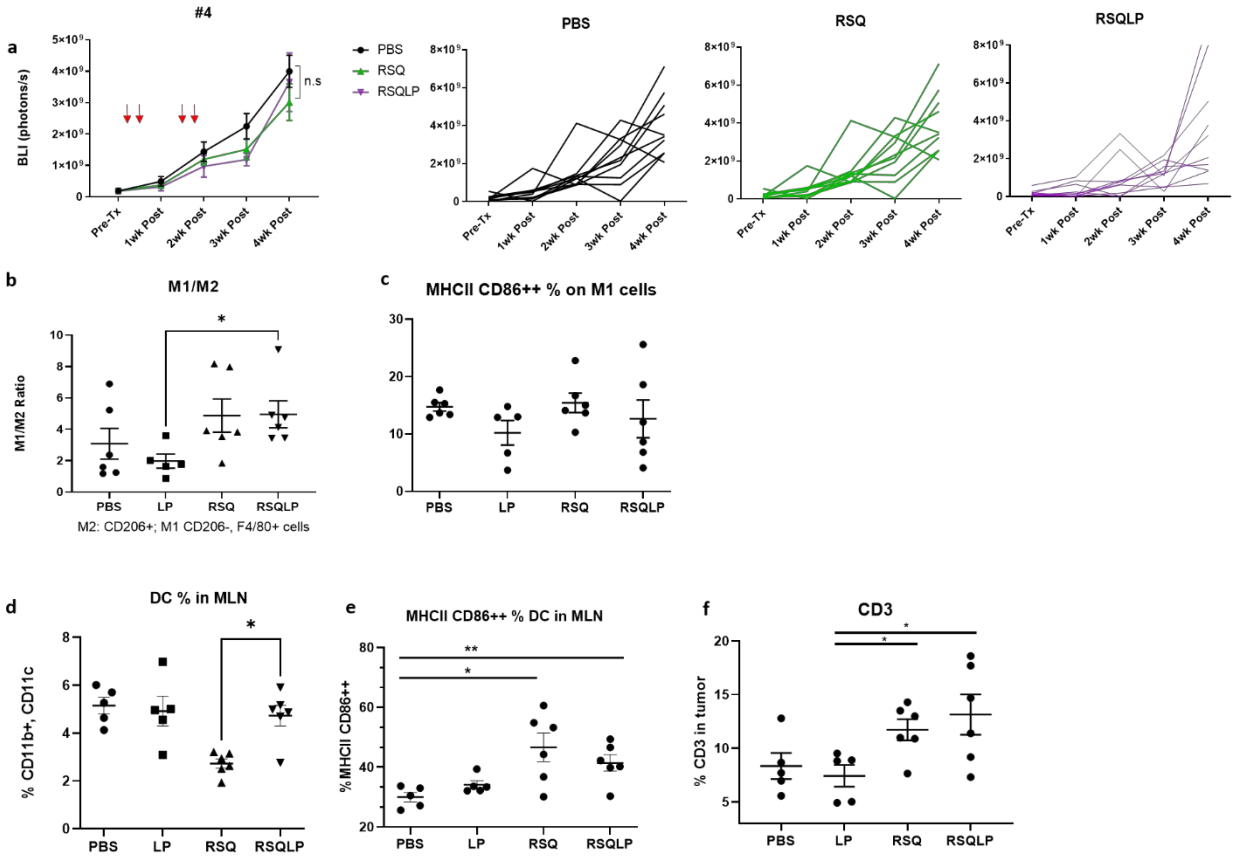

Figure S8. Bioluminescent imaging data (BLI) for in vivo efficacy of RSQ and RSQLP only in ID8 bearing C57BL6 mice and tumor immune phenotyping. *a)* Shown are summary plot for tumor growth curve for experiment #4. On the left are individual tumor growth bioluminescent data for each treatment groups. b) Flow cytometry analysis of M1/M2 ratio of macrophage in the tumor microenvironment and c) CD86, MHCII++ percentage on M1 cells. d) Percentage of CD11b+, CD11c+ dendritic cells in mesenteric lymph node, e) activation of dendritic cells (CD86, MHCII++) f) CD3+ T cell percentage in the tumor microenvironment (n=5 or 6).

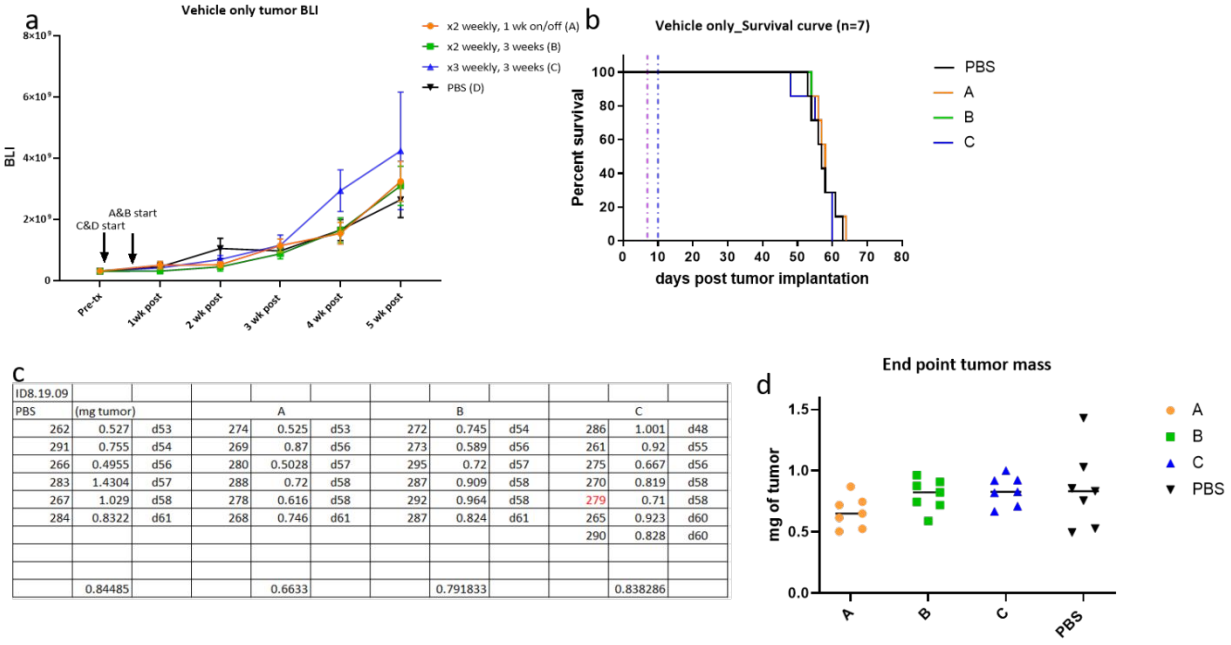

ID8.19.09											
PBS	(mg tumor)		A			B			C		
262	0.527	d53	274	0.525	d53	272	0.745	d54	286	1.001	d48
291	0.755	d54	269	0.87	d56	273	0.589	d56	261	0.92	d55
266	0.4955	d56	280	0.5028	d57	295	0.72	d57	275	0.667	d56
283	1.4304	d57	288	0.72	d58	287	0.909	d58	270	0.819	d58
267	1.029	d58	278	0.616	d58	292	0.964	d58	279	0.71	d58
284	0.8322	d61	268	0.746	d61	287	0.824	d61	265	0.923	d60
									290	0.828	d60
	0.84485			0.6633			0.791833			0.838286	

Figure S9. Vehicle only effect on ID8 tumor growth in C57BL6 mice. a) bioluminescent imaging data showing tumor growth kinetics for ID8 bearing mice that were treated with empty liposome based on different treatment plan. A. start on day 10 post tumor implantation, x2 per week, 1 week on week off; B. start on day 10 post tumor implantation, x2 per week for 3 week; C. start on day 7 post tumor implantation, x3 per week for 3 weeks). b) long term survival curve for ID8 bearing mice that were treated with empty liposomes, c. mice were euthanized based on endpoint criteria and tumors were collected for end point tumor burden, d. summary plot for end point tumor mass (n=7).

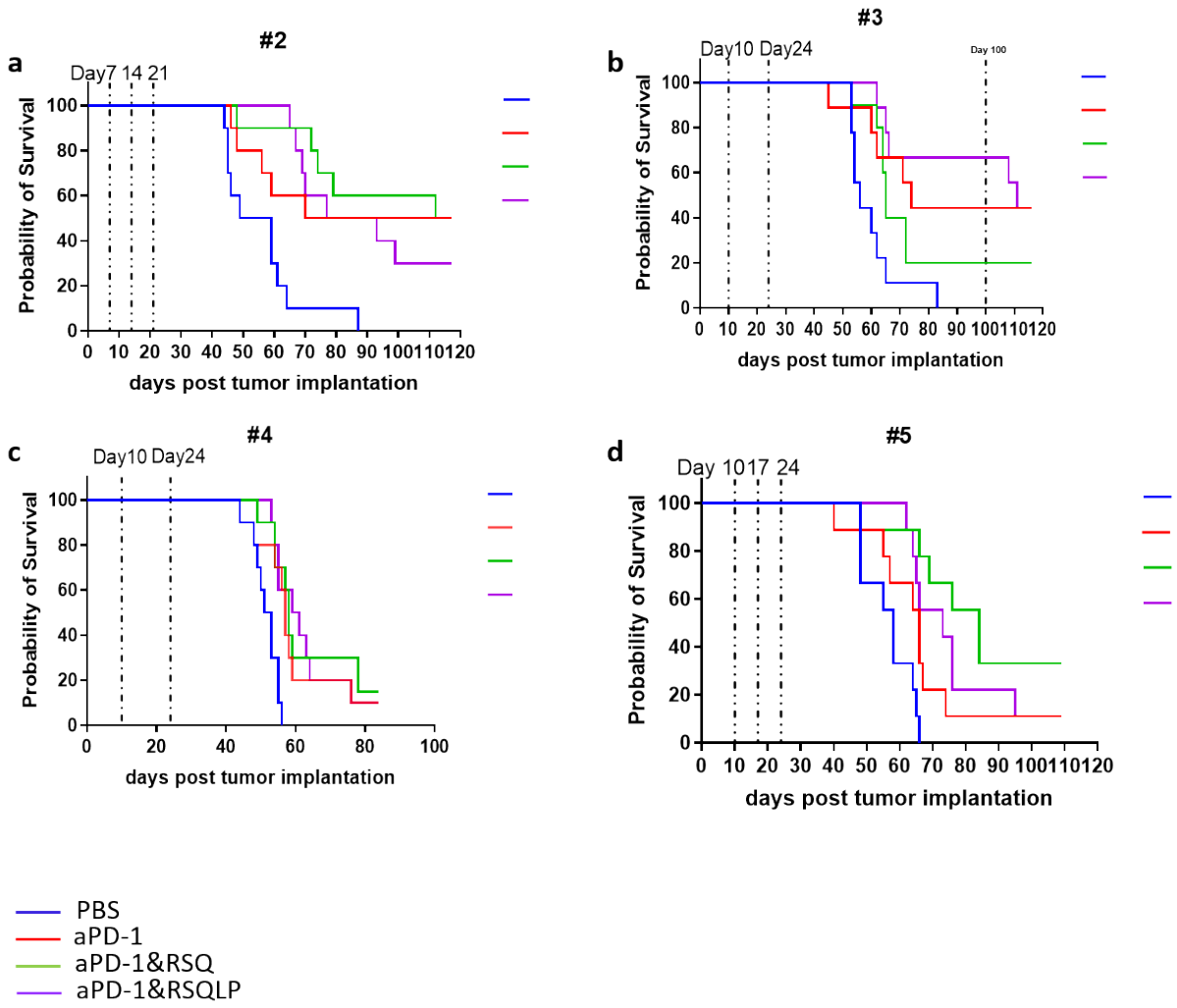

Figure S10. Kaplan Meier survival graph for experiments (#2-#5 see Table 1 for treatment details) (n=9 or 10 for each experiment).

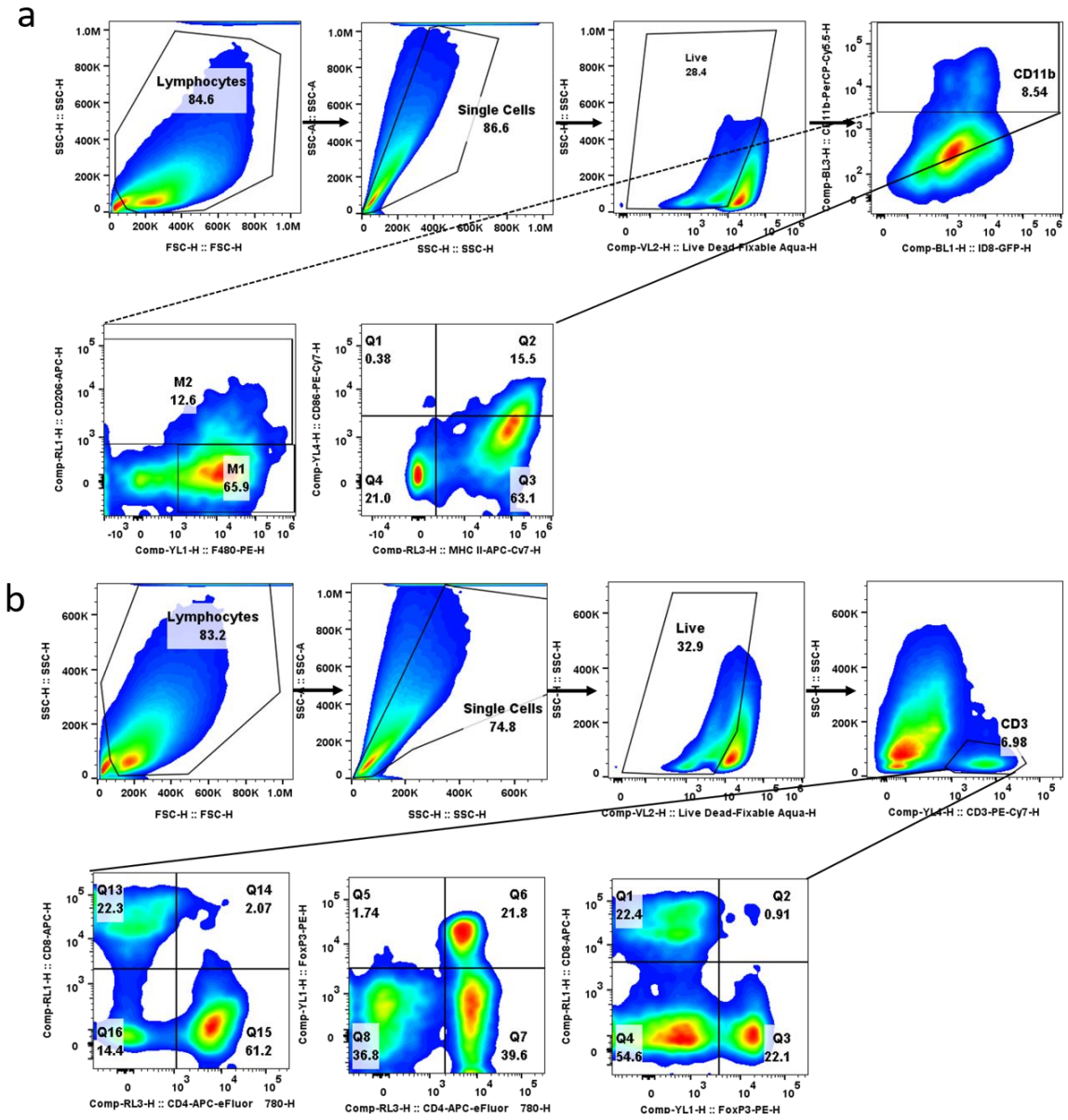

Figure S11. **Gating Strategy for flow cytometry analysis**. a) Figure 5a,b (M1/M2 macrophage analysis in ovarian tumor microenvironment b) Figure 5 c,d (tumor infiltrating lymphocyte analysis including CD4, CD8, FoxP3 lymphocyte population in ovarian tumor).

p values

Figure 5a

Welch's t test (unpaired t test, don't assume same SD)

M1		
LP	RSQ	0.001
LP	RSQLP	0.0004
PBS	RSQ	0.0388
PBS	RSQLP	0.0199

Figure 5b

M2		
LP	RSQ	0.0789
LP	RSQLP	0.0319
PBS	RSQ	0.2475
PBS	RSQLP	0.1146

Figure 5d

Welch's t test (unpaired t test, don't assume same SD)

CD8/Treg		
LP	RSQ	0.004
LP	RSQLP	<0.0001
PBS	RSQ	0.6331
PBS	RSQLP	0.0403
RSQ	RSQLP	0.0037

Figure 5e

% Treg		
LP	RSQ	0.0003
LP	RSQLP	<0.0001
PBS	RSQ	0.0999
PBS	RSQLP	0.0077
RSQ	RSQLP	0.0187

Figure 5f

Welch's t test (unpaired t test, don't assume same SD)

PD1 expression on CD3+ T cells		
LP	RSQ	0.2494
LP	RSQLP	0.0065
PBS	RSQ	0.7185
PBS	RSQLP	0.0829
RSQ	RSQLP	0.1538

Figure S6b

Welch's t test (unpaired t test, don't assume same SD)

M1/M2 ratio		
LP	RSQ	0.0435
LP	RSQLP	0.017
PBS	RSQ	0.2415
PBS	RSQLP	0.1829

Figure S6e

DC MHCII CD86++		
LP	RSQ	0.0464
LP	RSQLP	0.0448
PBS	RSQ	0.0158
PBS	RSQLP	0.0066

Figure S6f

Welch's t test (unpaired t test, don't assume same SD)

CD3		
LP	RSQ	0.0144
LP	RSQLP	0.0295
PBS	RSQ	0.0158
PBS	RSQLP	0.0634

Table S1. p values for immunophenotyping studies

Reference

1. Ghosn, E. E.; Cassado, A. A.; Govoni, G. R.; Fukuhara, T.; Yang, Y.; Monack, D. M.; Bortoluci, K. R.; Almeida, S. R.; Herzenberg, L. A.; Herzenberg, L. A., Two physically, functionally, and developmentally distinct peritoneal macrophage subsets. *Proceedings of the National Academy of Sciences of the United States of America* **2010,** *107* (6), 2568-73.